Original Paper

Neuro-Signals

Neurosignals 2012;20:86–102
DOI: 10.1159/000330805

Received: March 16, 2011
Accepted after revision: July 7, 2011
Published online: December 22, 2011

JNK/ERK/FAK Mediate Promigratory Actions of Basic Fibroblast Growth Factor in Astrocytes via CCL2 and COX2

Mathieu P. Lichtenstein[a, b] José L.M. Madrigal[f, g] Aurora Pujol[c–e] Elena Galea[a–c]

[a]Institut de Neurociències, [b]Departament de Bioquímica, Universitat Autònoma de Barcelona, [c]Institució Catalana de Recerca i Estudis Avançats, [d]Centre de Genètica Mèdica i Molecular, Institut d'Investigació Biomèdica de Bellvitge, Hospitalet de Llobregat, Barcelona, [e]Centro de Investigación Biomédica en Red de Enfermedades Raras, Valencia, [f]Departamento de Farmacología, Facultad de Medicina, Universidad Complutense de Madrid, y [g]Centro de Investigación Biomédica en Red de Salud Mental, Madrid, España

Key Words

Astrocyte · Basic fibroblast growth factor · c-jun N-terminal kinase · Cytoskeleton · Extracellular-signal-regulated kinase · Focal adhesion kinase · Intercellular adhesion molecule migration · Monocyte chemoattractant protein · Cyclo-oxygenase-2

Abstract

While the role of cytokines in causing pro- and anti-inflammatory cascades in the brain and that of chemokines in promoting chemotaxis is well recognized, the immunomodulatory actions of neurotrophins released during brain injury remains largely undetermined. This knowledge gap affects basic fibroblast growth factor (FGF2), which in the brain is mainly produced by astrocytes and characteristically upregulated in reactive astrocytes. The goal of this study was to characterize the inflammatory actions of FGF2 in astrocytes using primary cultures. We report that FGF2 induced the upregulation of monocyte chemoattractant protein (CCL2) and cyclo-oxygenase type 2 (COX2), and the inhibition of lipopolysaccharide-elicited ICAM1 upregulation. The effects of FGF2 were: (i) dependent on gene transcription as revealed by the concomitant regulation of CCL2 or ICAM1 mRNAs; (ii) mediated by the FGF2 receptor type 2; (iii) dependent on ERK, JNK and FAK, and (iv) NF-κB-independent. FGF2 also caused accelerated wound closure dependent on CCL2, COX2, ERK, JNK and FAK in a scratch assay. We conclude that the signaling network triggered by FGF2 in astrocytes converged into accelerating directed motion. It follows that astrocyte migration to injury sites may be a key factor in the repair mechanisms orchestrated by FGF2.

Introduction

Basic fibroblast growth factor (FGF2) is a ubiquitous and versatile peptide that regulates cell proliferation, migration, cell survival and differentiation during development, tissue repair or tumor growth. FGF2 is produced in several isoforms ranging between 18 and 34 kDa that are produced by alternative use of two initiation codons at translation [1]. The low-molecular-weight (LMW) isoform (18 kDa) is secreted [2, 3] by a mechanism implicating multidrug resistance-associated proteins [4] and Na^+/K^+-ATPase [4, 5], and accounts for most of the biological functions attributed to FGF2 by acting through membrane-spanning tyrosine kinase receptors in conjunction with low-affinity binding to heparin sulfate proteogly-

KARGER

Fax +41 61 306 12 34
E-Mail karger@karger.ch
www.karger.com

1424–862X/12/0202–0086$38.00/0

Accessible online at:
www.karger.com/nsg

Mathieu P. Lichtenstein, MD
Institut de Neurociències, Edifici M
Universitat Autònoma de Barcelona, Bellaterra
ES–08193 Barcelona (Spain)
Tel. +34 93 586 8142, E-Mail matlichtenstein@hotmail.com

cans [6]. In addition, LMW-FGF2 can exert nuclear actions upon internalization – alone or in complex with its receptors – and subsequent import to the nucleus [7–10]. Specific proteins like translokin [11], or importin [12] mediate the intracellular trafficking of FGF2 and fibroblast growth factor receptor (FGFR)-1, respectively. By contrast, high-molecular-weight FGF2 isoforms (21–25 kDa) are localized in the nucleus and cytoplasm and their function remains largely unknown, although some reports point to an implication in cell growth control [13, 14].

In the brain, FGF2 is a regulator of processes leading to tissue repair and regeneration after injury including scar formation [15], angiogenesis [16], neuronal survival [17] and recruitment of neuronal progenitors [18]. An often underappreciated fact in FGF2-dependent repair is that astrocytes are the primary source of the factor and, indeed, overexpression of FGF2 in reactive astrocytes is a hallmark of brain injury [18–21]. The terms 'reactive astrocytes' or 'gliosis' define the cellular hypertrophy that astrocytes undergo as part of the inflammatory reactions that follow brain injury, infection or degeneration. While the postinjury increase of FGF2 expression in astrocytes suggests a role of the factor in driving astrogliosis, it has never been examined whether FGF2 controls astrocyte inflammatory responses and, if so, what precise molecules and pathways are involved. A hint is provided by a preliminary study wherein the effect of axonal injury-associated factors in astrocyte migratory response was tested in a model of scratch injury in cultured astrocytes. LMW-FGF2 strongly stimulated astrocyte migration and this response was the greatest among all factors tested, which included transforming growth factor-β, epidermal growth factor and insulin-like growth factor [22]. Here we sought to further characterize the FGF2-elicited immunomodulation of astrocytes by focusing on the expression of molecules with a documented ability to regulate migration. These were monocyte chemoattractant protein (CCL2, formerly called MCP1), cyclo-oxygenase-2 (COX2) and intercellular adhesion molecule 1 (ICAM1). CCL2 is a potent chemoattractant and activator for monocytes, and is primarily expressed in astrocytes in ischemia and after peripheral administration of bacterial lipopolysaccharide (LPS) [23]. CCL2 plays a critical role in the migration of newly formed neuroblasts from neurogenic niches to damaged regions of the brain after focal ischemia [24]. ICAM1, in addition to its well-established control of leukocyte adhesion and migration across the blood-brain barrier [25, 26], is expressed in astrocytes in Alzheimer's disease and other neurodegenerative diseases [27], where it is believed to contribute to microglia recruitment [28]. COX2, in turn, is expressed in reactive astrocytes in neuropathological conditions [29, 30], and a wealth of evidence documents the capacity of COX2-released prostaglandins to increase cancer cell motility [31, 32]. The role of COX2 in astrocytes is, however, largely unknown. LPS was used as a positive control of inflammatory activation in astrocytes. We report that LMW-FGF2 stimulated the expression of CCL2 and COX2, whereas it decreased the LPS-induced ICAM1 expression, in astrocytes cultured from rat cerebella. FGF2 accelerated astrocyte migration in a scratch model in vitro, the effect being mediated by CCL2 and COX2 but not ICAM1. The actions of FGF2 were mediated by the FGF2 receptor type 2 (FGFR2) and JNK/FAK/ERK-dependent signaling. Cell proliferation did not contribute to this phenomenon because inhibitors of cell growth had no effect. We conclude that FGF2 induces a promigratory phenotype in astrocytes, which may be a key factor in the repair mechanisms orchestrated by FGF2 during brain injury.

Material and Methods

Materials

Recombinant human FGF2 was purchased from R&D Systems. Dulbecco's modified Eagle's medium (DMEM), penicillin, streptomycin, paraformaldehyde, Triton X-100, bovine serum albumin (BSA), cytosine-arabinoside, LPS, 4′,6-diamidino-2-phenylindole (DAPI), phosphatase inhibitors, mouse anti-actin (1/10,000) antibody, rabbit anti-FGFR1 and anti-FGFR2 (1/500), mouse anti-GFAP antibodies were obtained from Sigma. Protease inhibitors, PVDF membranes and LightCycler capillaries were from Roche. Reverse transcriptase and Taq Polymerase were purchased from Invitrogen. Fetal-bovine serum (FBS) was from Cambrex. Anti-COX2 (1/1,000) rabbit polyclonal antibody was from Cayman. Anti-CCL2 (1/500) rabbit polyclonal antibody was from Abcam. Anti-ICAM1 (CD54, clone 1A29) mouse monoclonal antibody and isotype matched IgG1 were purchased at BD Pharmingen, and anti-GAPDH and CREB antibodies from Santa Cruz. Primers and NF-κB oligonucleotides were synthesized by Roche. Rabbit monoclonal antibodies against ERK1/2 and phospho-ERK (pERK), JNK1/2 and phospho-JNK (pJNK), FAK and phospho-FAK (Tyr 397) were from cell signaling (all used a 1/1,000 dilution). Viral particles encoding shRNA for FGFR2, GFP, and rabbit anti-FGFR3 antibody were from Santa Cruz Biotechnology. ERK (PD98059), JNK (SP600125) and FAK (PF573228) inhibitors were from Tocris.

Astrocyte Cultures

Astrocyte cultures were prepared from cerebellum from 7- to 8-day-old Sprague-Dawley rats as described [33]. In brief, the rats were decapitated and their brains immediately dissected out. After meninges and blood vessels were removed, the tissue was minced and incubated for 10 min at 37°C in Ca^{2+}-free Krebs-Ringer buffer containing 0.025% trypsin. Cells were then mechanically triturated through a glass pipette and filtered through

a 40-μm nylon mesh in the presence of 0.52 mg/ml soybean trypsin inhibitor and 170 IU/ml DNase. After centrifugation (500 *g*), the cells were stained by Trypan blue exclusion, counted in a Neubauer chamber and then resuspended in 90% DMEM, 10% FBS, 20 U/ml penicillin and 20 μg/ml streptomycin at 6×10^5 cells/ml. The dishes used for each experiment were: 35-mm dishes for immunofluorescence and migration experiments, 48-well plates for ELISAs, 60-mm plates for Western blot and 100-mm plates for EMSA. The cells were maintained in a humidified atmosphere of 90% air-10% CO_2. The medium was changed at day 7 and the cells were immediately used when cultures reached confluency (around 12 DIV). This minimizes contamination by microglia, which rapidly proliferate when the astrocyte monolayer reaches confluency [33]. To quantify microglia, cultures were incubated with DiL-Ac-LDL (Molecular Probes) 10 μg/ml for 2 h, which is readily taken up by microglia [34], and counterstained with DAPI to label the nuclei and thereby obtain the total number of cells. The percentage of DiL-Ac-LDL-positive cells with respect to the total number of cells was 10.74 ± 4.09% (n = 4).

The medium was changed to 1% FBS-DMEM overnight before treating the cultures with different compounds for the indicated times and concentrations to minimize cell proliferation. Cerebellar granule cells were obtained by the same protocol as astrocytes but were seeded at 1.3×10^6 cells/ml in the same culture media as astrocytes. At day 1 in vitro, cytosine arabinoside (10 μM) was added to prevent glia proliferation. Cell lines 3T3s, HeLa and SH-SY5Y were passaged every 3–4 days and cultured in 90% DMEM, 10% FBS, 20 U/ml penicillin and 20 μg/ml streptomycin, except for SH neuroblastoma that were cultured in 20% FBS.

Immunocytochemistry

The cultures were fixed for 30 min with 4% paraformaldehyde in phosphate-buffered saline (PBS) at room temperature. After several washes, the monolayers were incubated with PBS-0.1% Triton X-100 for 15 min to permeabilize the cells. This permeabilization step was omitted in the case of ICAM as this protein is extracellular. A blockade of nonspecific binding was performed with 1% BSA in PBS, and afterwards the cells were incubated overnight at 4°C with mouse monoclonal anti-GFAP (1/1,000), rabbit anti-CCL2 (1/3,000), anti-COX2 (1/500) or anti-ICAM1 (1/200) antibodies in 0.1% BSA-PBS. After washing, the cells were incubated for 1 h with Alexa-labeled secondary IgGs diluted 1/1,000 in 0.1% BSA-PBS. The primary antibody was omitted in the controls. In the last wash, the cells were incubated with DAPI to perform nuclear staining.

CCL2 ELISA

After the indicated treatment, CCL2 levels in the culture medium were assessed using an ELISA specific for rat CCL2 according to the manufacturer's instructions (R&D Systems). The assay detection limits were 30–2,000 pg/ml.

ICAM1 ELISA

ELISAs were performed as thoroughly described elsewhere [35]. In brief, the cells were fixed with 4% paraformaldehyde in PBS and incubated overnight with a monoclonal antibody against rat ICAM1 (clone 1A29, Pharmingen; concentration 3 μg/ml). Isotype-matched IgG1κ (Pharmingen) was used at the same concentration as the negative control. The cells were finally incubated with a goat anti-mouse antibody conjugated to alkaline phosphatase (1:1,000; Sigma). The alkaline phosphatase substrate was added, and the cells incubated at room temperature until the reaction developed. The OD_{405} was measured in a Bio-TeK PowerWave XS microplate spectrophotometer.

Real-Time PCR

Total RNA was prepared from cells using the Trizol reagent (GIBCO). Aliquots (0.5–1.0 μg) were converted to cDNA (SuperScript II, Invitrogen) using random hexamer primers and mRNA levels estimated by real time, quantitative RT-PCR (Q-PCR). The primers used were: CCL2 fwd: 5′-CTTCTGGGCCTGTTGTTCAC-3′, CCL2 rvs: 5′-GGGACGCCTGCTGCTGGTGATTC-3′; ICAM1 fwd 5′-GGGCCCCCTACCTTAGGAA-3′, ICAM1 rvs 5′-GGGACAGTGTCCCAGCTTTC-3′; 18S fwd 5′-GGGAGGTAGTGACGAAAAATAACAAT-3′, 18S rvs 5′-TTGCCCTCCAATGGATCCT-3′. The cycling conditions were: 35 cycles of denaturation at 94°C for 30 s, annealing at 58°C for 30 s and extension at 72°C for 30 s, followed by 2 min at 72°C, in the presence of SYBR Green (1:10,000 dilution of stock solution from Molecular Probes, Eugene, Oreg., USA). The reactions were carried out in a 20-μl reaction volume in a LifeCycler (Roche). Relative mRNA concentrations were calculated from the take-off point (Ct) of the PCR reactions and normalized for the levels of 18S ribosomal RNA using the software provided by the manufacturer. Correct product amplification was confirmed by the existence of a single melting point in melting curve analysis and by size determination using 2% agarose gel electrophoresis.

Preparation of Cytosolic and Nuclear Extracts

After treatment, the cells were scraped out of the plates in ice-cold PBS, collected by brief centrifugation, resuspended in buffer A containing 10 mM HEPES pH 7.9; 1.5 mM $MgCl_2$, 10 mM KCl, 0.5 mM dithiothreitol and a cocktail of protease (Roche) and phosphatase (Sigma) inhibitors. Nonidet P-40 was added (final concentration 0.6%) and the cells vortexed for 10 s. The nuclei were collected by brief centrifugation in a microcentrifuge and the supernatants kept at –80°C as cytosolic extracts. The nuclei were washed once with buffer A and collected again by centrifugation. Nuclear extracts were obtained by incubating nuclei in buffer B (20 mM HEPES buffer pH 7.6, 25% glycerol, 420 mM NaCl, 0.2 mM ethylenediaminetetraacetic acid (EDTA), 0.5 mM dithiothreitol, and protease and phosphatase inhibitors) at 4°C for 30 min with gentle rocking. The suspensions were centrifuged at 15,000 *g* for 15 min at 4°C and the supernatants stored at –80°C. Protein concentrations were measured by the Bradford method.

Western Blot

Samples containing equal amounts of protein (15–30 μg) were subjected to sodium dodecyl sulfate-polyacrylamide gel electrophoresis on 8–15% gels. The proteins were then transferred to polyvinyl difluoride membranes, which were blocked with 5% milk in Tris-buffered saline containing 0.1% Tween-20 for 1 h and incubated overnight at 4°C with primary antibodies (indicated in 'Materials'). This was followed by incubation with anti-IgG-horseradish peroxidase-labeled secondary antibodies (Pierce, 1/10,000) for 1 h at room temperature and subsequent detection with an enhanced chemiluminescence detection kit (ECL, Amersham Life Science). Proteins were visualized by autoradiography on X-ray film (AGFA) and the relative band intensity was quantified with Image J (National Institutes of Health).

Electrophoretic Mobility Shift Assays

Electrophoretic mobility shift assays were performed as thoroughly described previously [35]. In brief, the NF-κB oligonucleotides corresponding to the palindromic consensus sequences were end-labeled with 10 μCi [γ^{32}P-ATP] (Amersham) with 10U T4 polynucleotide kinase (Fermentas) and purified in G-25 Sephadex columns (Sigma). Nuclear extracts (5–10 μg protein) were incubated with radiolabeled oligonucleotides in a final volume of 20 μl in the presence of 1 μg poly dIdC, 20 mM HEPES buffer pH 7.9, 1 mM EDTA, 5% glycerol, 100 mM NaCl and 0.5 mM dithiothreitol. DNA-protein complexes were resolved by electrophoresis in 4% nondenaturing polyacrylamide gels using 0.5 × Tris-borate-EDTA as the running buffer. Autoradiographs were obtained by placing dried gels in close contact with films (AGFA).

Retroviral Infection

Viral particles encoding for rat shRNA FGFR2 were purchased from Santa Cruz Biotechnology. Preconfluent cultures (DIV 6–7) were infected with 2 × 10^4 retroviral particles per ml overnight in 10% FBS containing DMEM, and were grown for 7 days to confluency to permit integration and expression of shRNAs. The efficiency of FGFR2 silencing was confirmed by Western blotting. GFP-expressing (Santa Cruz) viruses were used as a control for efficient infection.

Scratch Wound Assay

The capacity of astrocytes to migrate was tested by scratching confluent astrocyte monolayers to induce natural cell migration to close the scratch, as previously reported [36]. The scratch was 500 μm wide and 35 mm long, and was done with a sterile yellow pipette tip. The cells were treated immediately after scratching and pharmalogical inhibitors, when indicated, were present the entire time. In some cases blocking/activating antibodies were used as follows: anti-CCL2 4 μg/ml, anti-ICAM1 10 μg/ml and unspecific isotype-matched IgG1 antibody (as control) 10 μg/ml, which were also present during the entire length of the migration experiments. The cells were fixed at 0–24 h thereafter, and immunostained for GFAP/DAPI and/or COX2, CCL2 or ICAM. Individual images (6 per scratch-wound) were taken with ×2 magnification and the cell-free area was measured using ImageJ Software.

Statistical Analysis

The experiments were always reproduced a minimum of 3 times. Quantifiable determinations were expressed as means ± SEM of the indicated number of experiments performed in independent cultures. The significance of differences was evaluated by one-way ANOVA followed by the Newman-Keuls post-hoc test when more than 2 conditions were evaluated.

Results

FGF2 Modulated the Expression of CCL2, ICAM1 and COX2 in Astrocytes

The joint evaluation of CCL2 by ELISAs of culture media (fig. 1a–c), immunocytochemistry (fig. 1d), Western blots of whole cells (fig. 1e), and RT-PCR (fig. 1f) indicated that FGF2 caused expression of the CCL2 gene and protein, and the release of the latter to the extracellular media. CCL2 was barely detectable in control cells by any approach. The increased CCL2 expression appeared to derive from *de novo* synthesis as judged by the robust perinuclear immunolabeling in the Golgi apparatus (fig. 1d). The effect of FGF2 was time and dose dependent (fig. 1a, b). CCL2 was thus detected in the extracellular media as early as 6 h after the administration of FGF2, and the chemokine contents increased progressively up to 48 h, the last time they were analyzed. When assessed at 24 h, the extracellular CCL2 increased linearly upon exposure to 5–100 ng/ml FGF2. The factor was hence used in the ensuing experiments at the submaximal dose of 25 ng/ml. Overall, the ELISAs appeared more sensitive than Western blots to quantify CCL2 production. Plausibly, the secretion of newly synthesized CCL2 diminishes the intracellular pool detected by Western blot. Considering that FGF2 is produced in the brain during the inflammatory reactions that follow injury, we also examined whether the increased production of CCL2 was enhanced when provoking a standard inflammatory condition by LPS. As previously reported [37], LPS caused expression of the CCL2 gene and protein in astrocytes (fig. 1c, e, f). LPS moderately increased the FGF2-elicited expression of CCL2, indicating additive rather than synergistic actions of both factors. The combined effect was evident at early (i.e. 5–12 h) but not late (i.e. 48 h) treatment times (fig. 1c, e, f) suggesting a detrimental effect of excess costimulation.

FGF2 also caused the transient expression of COX2 in astrocyte cultures (fig. 2) with a peak at 8 h, as revealed

(For figure see next page.)

Fig. 1. FGF2-induced CCL2 expression in astrocytes. **a–c** ELISA measurements of CCL2 in extracellular media: dose response (**a**); time course (**b**); effect of LPS (**c**); immunocytochemistry images being representative of at least 3 independent experiments and showing perinuclear localization of CCL2, presumably in the Golgi apparatus (**d**); Western blot analysis of whole-cell extracts showing a representative gel and densitometries (**e**), and RT-PCR analysis at 5 h (top) and 48 h (bottom) after the addition of FGF2 and/or LPS (**f**). The astrocytes were incubated with FGF2 (5–100 ng/ml in **a** and 25 ng/ml in the rest of the panels) or LPS (10 ng/ml) for 3–48 h. Values are the means ± SEM, of n = 3–5 independent experiments. * $p < 0.05$, ** $p < 0.01$ and *** $p < 0.001$, against control condition (no FGF2, no LPS), and $^{\#\#}$ $p < 0.01$, $^{\#\#\#}$ $p < 0.001$ against LPS-treated cultures at the same time of analysis. ANOVA analysis, Newman-Keuls post-hoc were used. FGF2 caused the *de novo* synthesis of CCL2 mRNA and protein, which was released. FGF2 moderately potentiated the LPS-elicited increase of CCL2 expression at early (i.e. 12 h) but not late times (i.e. 48 h). Scale bar was 50 μm.

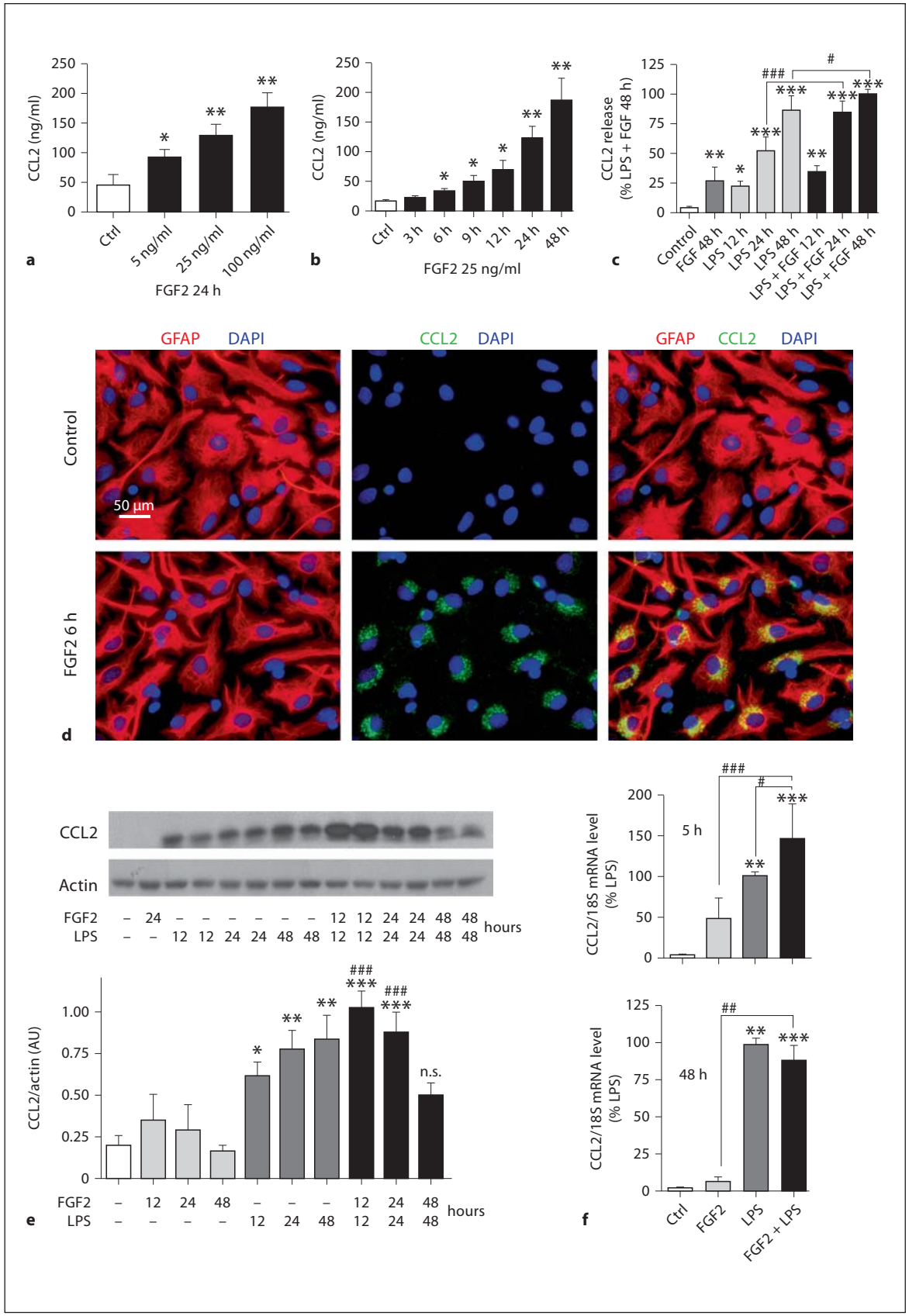
Color version available online
a
CCL2 (ng/ml)
Ctrl
5 ng/ml
25 ng/ml
100 ng/ml
FGF2 24 h
b
CCL2 (ng/ml)
Ctrl
3 h
6 h
9 h
12 h
24 h
48 h
FGF2 25 ng/ml
c
CCL2 release (% LPS + FGF 48 h)
Control
FGF 48 h
LPS 12 h
LPS 24 h
LPS 48 h
LPS + FGF 12 h
LPS + FGF 24 h
LPS + FGF 48 h
d
GFAP DAPI
CCL2 DAPI
GFAP CCL2 DAPI
Control
FGF2 6 h
50 µm
e
CCL2
Actin
FGF2
LPS
hours
CCL2/actin (AU)
n.s.
f
5 h
48 h
CCL2/18S mRNA level (% LPS)
Ctrl
FGF2
LPS
FGF2 + LPS

1

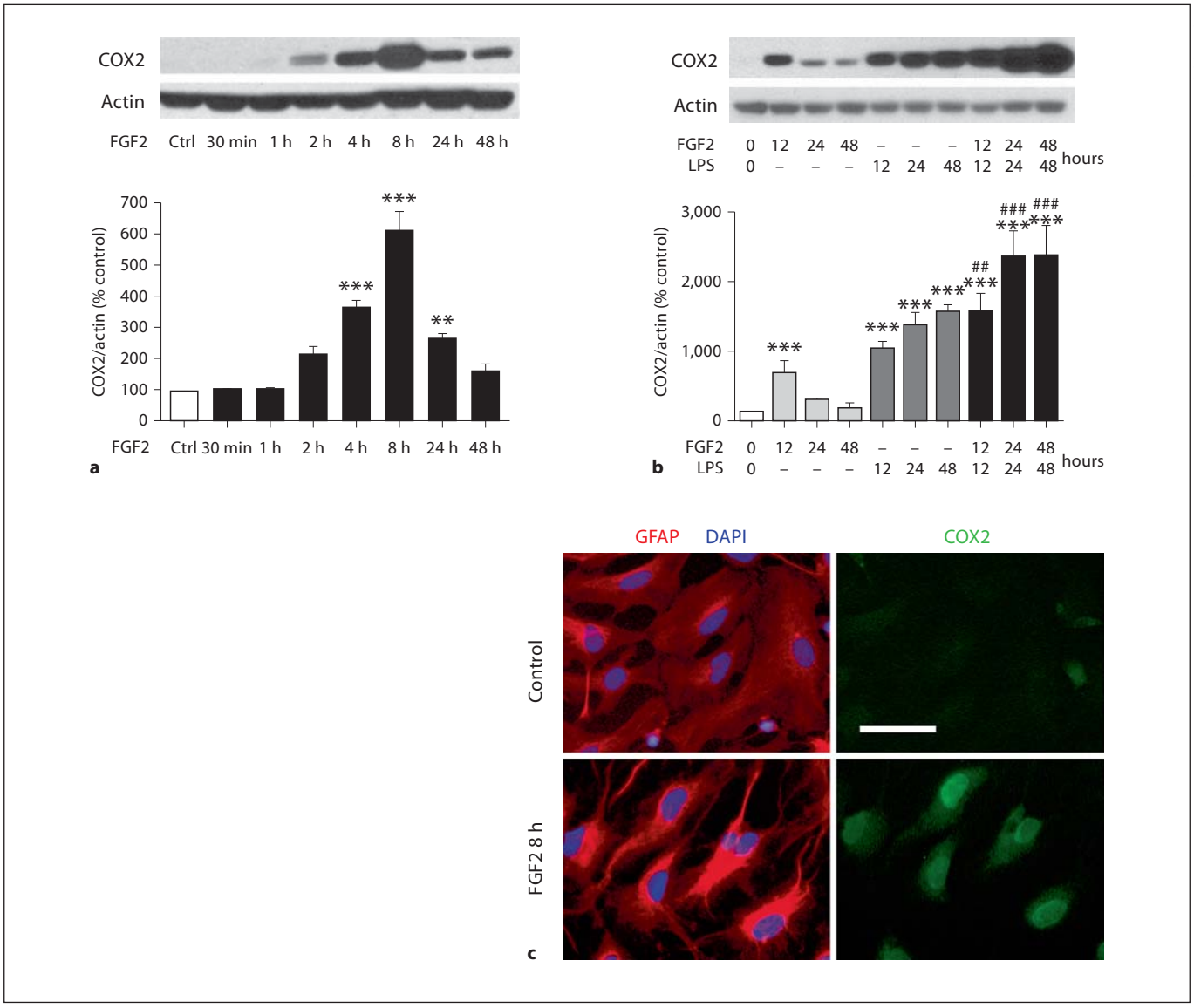

Color version available online

Fig. 2. FGF2 increased the expression of COX2. Western blot analysis showing a representative gel and densitometry (**a**); effect of costimulation with LPS assessed by Western blot (**b**), and immunocytochemistry representative of at least 3 independent determinations (**c**). The astrocytes were incubated with FGF2 (25 ng/ml) and/or LPS (10 ng/ml) for 0.5–48 h as indicated. Values are the means ± SEM of n = 4 independent experiments. ** $p < 0.01$, *** $p < 0.001$, with respect to controls, and ## $p < 0.01$, ### $p < 0.001$, with respect to LPS-treated cultures at the same time of analysis. ANOVA analysis, Neumann-Keuls post-hoc were used. Scale bar was 50 μm. FGF2 caused a transient expression of COX2 protein (maximal effect detected at 8 h) and LPS potentiated this increase.

by Western blot (fig. 2a). The immunocytochemical analyses confirmed that the increased expression originated in astrocytes and revealed, surprisingly, that part of COX2 was localized to the nucleus (fig. 2c), suggesting heretofore undescribed nuclear actions of the enzyme. Of note, FGF2 caused a morphological change in astrocytes consisting of soma retraction followed by process emission. The change, which has been previously reported and characterized [38], was clearly in progress 8 h after the addition of the factor. As compared with FGF2, LPS caused a more sustained increase of COX2 expression and potentiated the effect of FGF2 (fig. 2b).

Cells displayed a slight basal expression of ICAM1, detected by both ELISA (fig. 3a) and immunocytochemis-

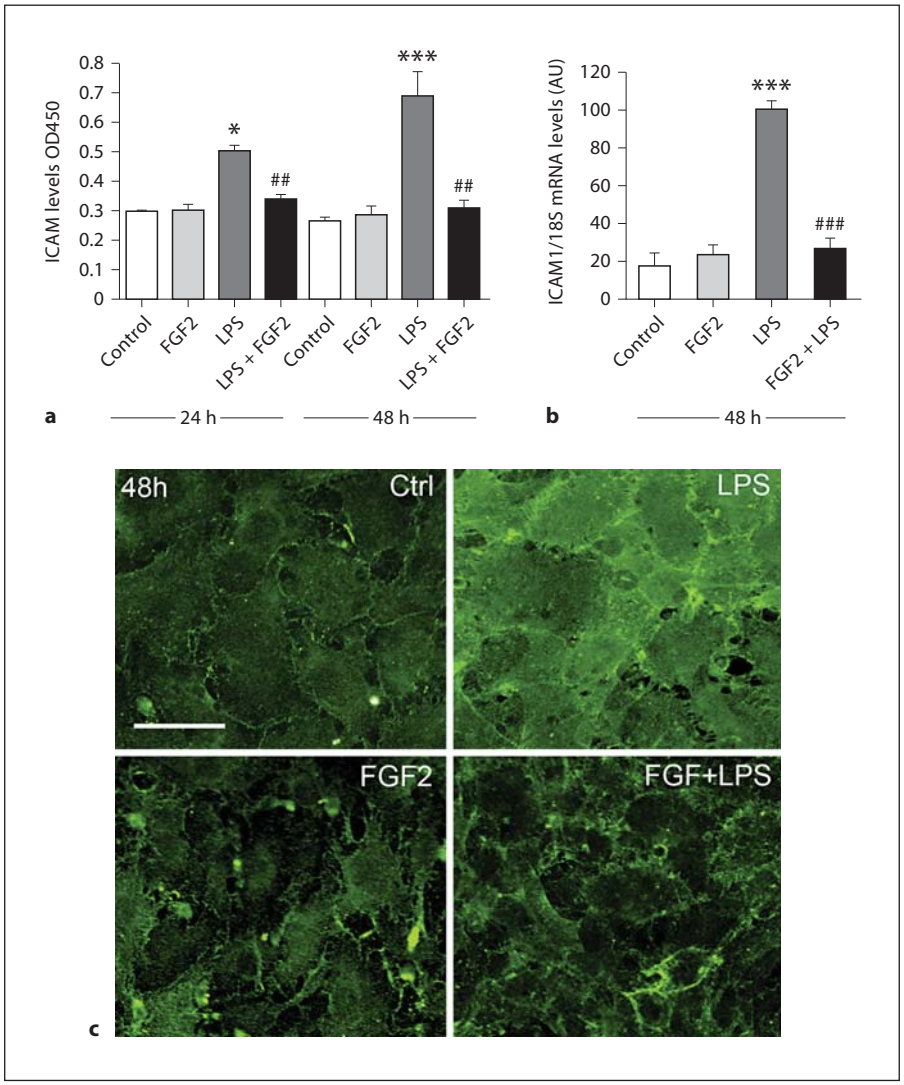

Fig. 3. FGF2 inhibited the LPS-elicited increase in ICAM1 protein and mRNA expression. ELISA (**a**); RT-PCR (**b**), and immunocytochemistry showing results representative of 3 independent experiments (**c**). The astrocytes were incubated with FGF2 (25 ng/ml) and/or LPS (10 ng/ml) for 24–48 h as indicated. Values are the means ± SEM of n = 4 independent experiments. * $p < 0.05$, *** $p < 0.001$, with respect to controls, and $^{\#\#}$ $p < 0.01$, $^{\#\#\#}$ $p < 0.001$, with respect to LPS-treated cultures at the same time of analysis. ANOVA analysis, Neumann-Keuls post-hoc were used. Scale bar = 50 μm.

try, which revealed that ICAM was localized to cell-to-cell contacts following a pattern reminiscent of a beehive (fig. 3c). FGF2 had no effect per se on ICAM1 expression, although it completely inhibited the increase of ICAM1 mRNA and protein caused by LPS (fig. 3b, c). The data indicated that FGF2 can exert both pro- or anti-inflammatory actions in astrocytes and that the anti-inflammatory effects (i.e. ICAM1 downregulation) were only manifest when additional inflammatory stimulation was performed as with LPS.

ERK, JNK and FAK but Not NF-κB Mediated the Immunomodulatory Actions of FGF2

FGF2 has been reported to activate numerous signal transduction pathways including MAPK (ERK, JNK, p38), PKC, PI3K-Akt, PKA, PKG and calcium-calmodulin kinase IV [39]. We sought proof of the participation of these kinases by determining: (i) whether specific inhibitors reversed the immunomodulatory actions of FGF2, using CCL2 as the endpoint in preliminary screens, and (ii) if FGF2 stimulated the pathways, which was assessed by Western blot analyses. Both requirements were only met by ERK and JNK, as documented below, while pharmacological inhibitors of p38, PKC, Akt, PKA or PKG had no effect (data not shown). Inhibitors of ERK (PD98059) and JNK (SP600125) completely inhibited the increase in CCL2 release (fig. 4a) and reversed the inhibition of ICAM1 caused by FGF2 back to 'LPS-*plus*-inhibitors' controls (fig. 4b). These values were slightly reduced as compared with the

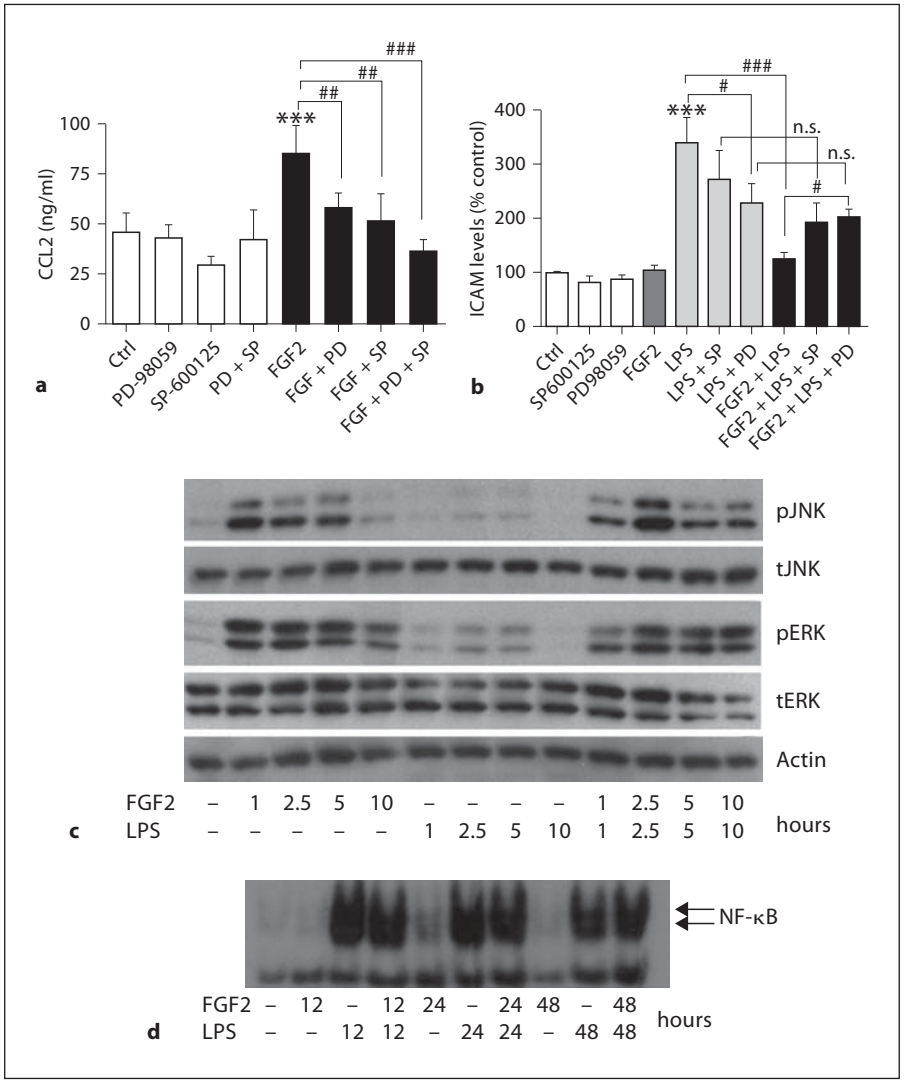

Fig. 4. The immunomodulatory actions of FGF2 were mediated by ERK and JNK but not NF-κB. Effect of PD98059 (ERK inhibitor) and SP600125 (JNK inhibitor) on the expression of CCL2 measured by ELISA at 24 h (**a**); effect of PD98059 and SP600125 on ICAM1 expression measured by ELISA at 48h (**b**); Western blot analysis of ERK and JNK phosphorylations showing a representative blot (**c**), and electrophoretic mobility shift assay analysis of NF-κB nuclear translocation (**d**). Arrows point to NF-κB complexes of different electrophoretic mobility. Astrocytes were incubated with 25 ng/ml FGF2 (and 10 ng/ml LPS in the case of ICAM1 and NF-κB). Cells had been preincubated for 1 h with PD98059 (50 μM) or SP600125 (10 μM) before the addition of factors. FGF2 activated ERK and JNK-dependent pathways to a much greater extent than LPS, and ERK and JNK pharmacological inhibitors reversed the actions of FGF2. LPS caused a long-lasting activation of NF-κB that was not mimicked nor modified by FGF2. Values are means ± SEM of n = 3–5 independent experiments. *** $p < 0.001$, with respect to controls, and $^{\#}$ $p < 0.05$, $^{\#\#}$ $p < 0.01$ and $^{\#\#\#}$ $p < 0.001$, with respect to FGF2- or LPS-treated cultures. n.s. = Not significant. ANOVA analysis followed by Neumann-Keuls was used. ERK/JNK and NF-κB blots are representative of at least 3 independent determinations.

ICAM1 expression attained with LPS alone (fig. 4b). FGF2 caused the phosphorylation of both ERK and JNK, which was detected as early as 1 h after the administration of the factor and persisted over the next 5 h (fig. 4c). Interestingly, LPS caused a small, barely detectable increase of pERK and pJNK and did not significantly alter the increases elicited by FGF2 (fig. 4c). This is in accordance with the small inhibitory effect of ERK and JNK inhibitors detected in the LPS-elicited ICAM upregulation. By contrast, electrophoretic mobility shift assay analysis showed a strong and long-lasting activation of NF-κB upon LPS administration (fig. 4d). NF-κB was thus present in the nucleus of LPS-treated astrocytes as soon as 30 min after treatment (data not shown), and remained activated for at least 48 h. FGF2 neither activated NF-κB per se nor interfered with the LPS-mediated activation of the transcription factor. The immunomodulatory effects of FGF2 were hence NF-κB independent. Overall, the data support the notion that immunomodulatory regulation by LPS and FGF2 encompasses different signaling pathways. Finally, the JNK inhibitor SP600125, but not the ERK inhibitor PD98059, completely abrogated COX2 expression, indicating a role of JNK but not ERK in the upregulation of COX2 by FGF2 (fig. 5a).

Because studies exist documenting a strong interplay between ERK and FAK in directed cell movement [40], we also examined the role of FAK in the immunomodulatory effects of FGF2. The FAK inhibitor PF573238 completely inhibited COX2 (fig. 5a) and CCL2 (fig. 5b)

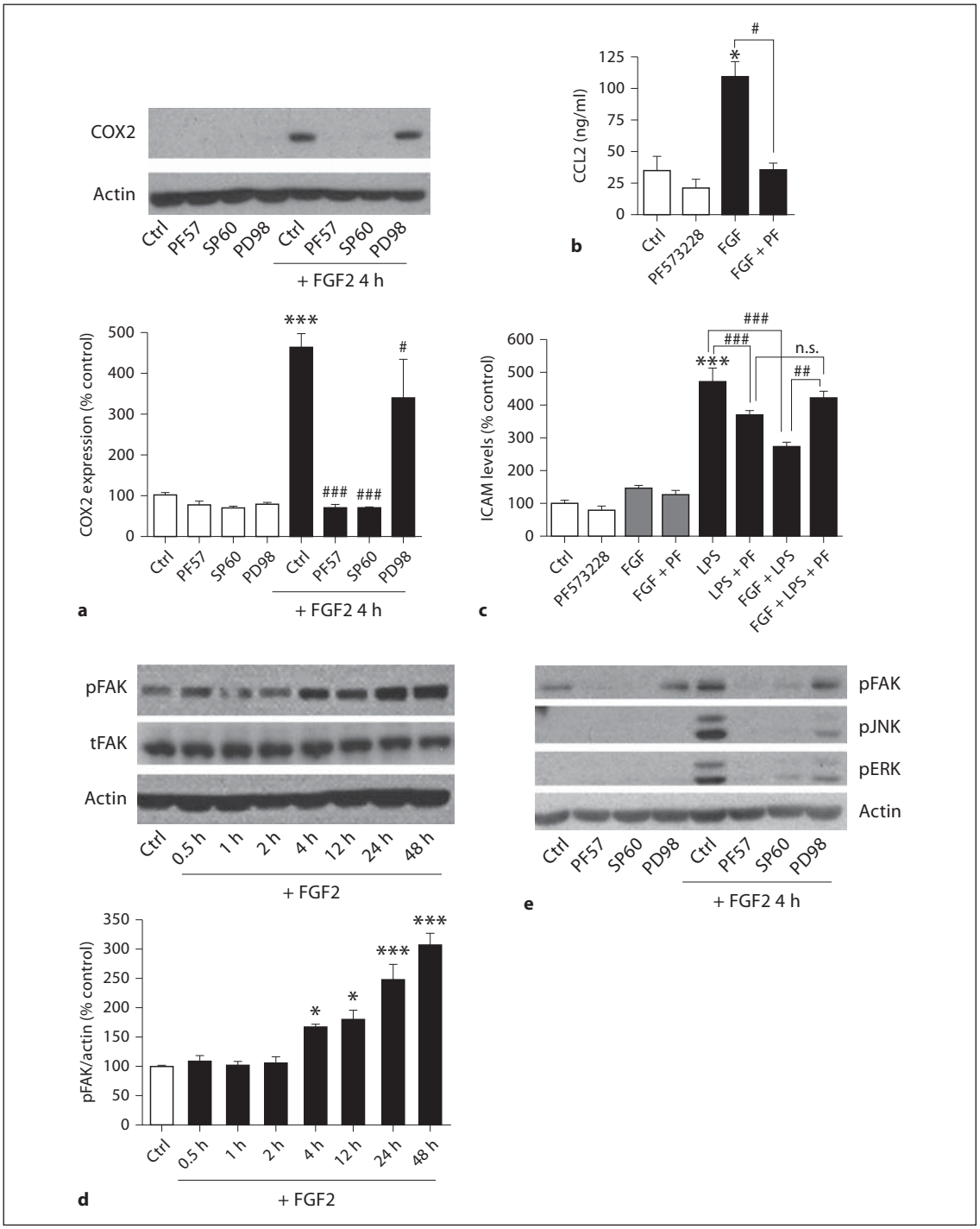

Fig. 5. The immunomodulatory actions of FGF2 were mediated by FAK. Western blot analysis of the effect of PD98059 (ERK inhibitor), SP600125 (JNK inhibitor) and PF573238 (FAK inhibitor) on the expression of COX2, showing a representative blot (top) and a densitometry (bottom) (**a**); effect of PF573238 on the secretion of CCL2 measured by ELISA (**b**); effect of PF573238 on ICAM1 expression measured by ELISA (**c**); Western blot analysis of FAK phosphorylation showing a representative blot and densitometry (**d**), and Western blot analysis of the interplay between ERK, FAK and JNK showing a representative blot (**e**). Astrocytes were incubated with 25 ng/ml FGF2 (and 10 ng/ml LPS in the case of ICAM1). Cells had been preincubated for 1 h with PD98059 (50 μM), SP600125 (10 μM) or PF573238 (2.5 μM) before the addition of factors. Values are means ± SEM of 3 independent experiments, except for **e** that shows results representative of at least 3 independent determinations. * $p<0.05$, ** $p<0.01$, *** $p<0.001$ against control conditions; # $p<0.05$, ### $p<0.001$ against FGF2 or LPS alone. ANOVA analysis followed by Neumann-Keuls were used.

upregulation, and reversed the inhibition of ICAM1 up to the 'LPS-*plus*-PF573238' control (fig. 5c). Accordingly, FGF2 caused activation of FAK, as judged by the increased pFAK, which was clearly detected 4 h after the addition of the factor and lasted for the ensuing 48 h (fig. 5d). We next examined the possible interplay between ERK, JNK and FAK by testing the effect of pharmacological inhibitors on kinase phosphorylations at 4 h after the administration of FGF2. PF573238 completely inhibited ERK and JNK stimulation, whereas SP600125 completely inhibited FAK and ERK (fig. 5e). By contrast, PD98059 inhibited JNK but not FAK (fig. 5e), indicating that ERK is downstream of the other two kinases. A model reconciling these findings is depicted in figure 8.

FGFR2 Mediated the Immunomodulatory Actions of FGF2

We next sought to identify the FGF2 receptor involved. We first determined whether astrocytes expressed FGFR1, FGFR2 or FGFR3 by Western blot analysis. Cerebellar granule cells (CGCs), C6 glioma, SHSY-5Y neuroblastoma, HeLa and NIH3T3 cell lines were used as positive controls. FGFR3 was highly expressed in C6, SHSY-5Y, HeLa and NIH3T3, while FGFR1 was detected in both C6 glioma and NIH3T3, but FGFR2 only in NIH3T3 (fig. 6a). Of the three receptors, only FGFR2 was detected in astrocytes (fig. 6a), where it appeared in the blots as two differently migrating bands that apparently arise from receptor glycosylation [41, 42]. Interestingly, exposure to FGF2 caused FGF2R to transiently disappear within 6–12 h after the addition of the factor (fig. 6b). The comparison of FGFR2 expression in cytosolic and nuclear fractions indicated that the receptor did not migrate to the nucleus (fig. 6c). The finding supports instead that the receptor was degraded after the exposure of astrocytes to FGF2.

Overall, the results pointed to FGFR2 as the receptor mediating the immunomodulatory effects of FGF2 in astrocytes. To establish this further, we tested whether astrocytes became unresponsive to FGF2 when obliterating FGFR2 expression by RNA interference. Activation of ERK and JNK pathways – assessed by the phosphorylation of the kinases – was used as the endpoint. Lentivirally-induced expression of FGFR2 shRNA in astrocytes reduced the expression of FGFR2, hence validating the gene-silencing approach (fig. 6d). FGFR2 shRNA inhibited the activation of ERK and JNK by FGF2 (fig. 6e).

FGF2-Mediated Migration

FGF2 has been shown to promote migration of astrocytes in a scratch-wound injury [22]. Here, we sought to establish whether the signaling pathways described above played a role in this phenomenon. First, we confirmed that FGF2 accelerated scratch closure (fig. 7a). The effect was not due to cell proliferation because the proliferation inhibitor cytosine arabinoside had no effect (fig. 7a). Rather, increased astrocyte polarity appeared to account for the acceleration, as revealed by the long protruding edges assembled in parallel in the moving fronts of FGF2-treated astrocytes (fig. 7b). We next tested the implication of the pathways regulated by FGF2 by interfering with their actions. We thus inhibited ERK, FAK, JNK and COX2 with the pharmacological inhibitors PD98059, PF573238, SP600125 or NS398, respectively. Specific antibodies were used to block the released CCL2 [43] or to stimulate ICAM1 [26], thereby reversing the dual, opposite actions of FGF2 on chemokine and adhesion molecule expression. The increased migration was completely abrogated by ERK, FAK and JNK inhibitors (fig. 7c). Likewise, blockade of CCL2 or COX2 reversed the increased migration with no effects on the controls (fig. 7d). By contrast, the antibody against ICAM1 had no effect (fig. 7d). In accordance with the effects of pharmacological inhibitors or modulatory antibodies, robust CCL2 and COX2 upregulation was detected in FGF2-treated astrocytes all over the cultures, not just near the migration fronts (fig. 7e), whereas no change was observed for ICAM1 expression (data not shown). Note that the picture in figure 7e was taken at 6 h after the administration of FGF2 to facilitate the detection of intracellular CCL2, at which time the morphological changes produced by the factor or the injury were not yet very pronounced. Incidentally, LPS had no effect on astrocyte migration (data not shown).

Discussion

We have shown here that LMW-FGF2 induced the upregulation of CCL2 and COX2 in astrocytes, while it completely antagonized the upregulation of ICAM1 caused by LPS. The data thus support an immunomodulatory rather than a proinflammatory or anti-inflammatory role of FGF2 in astrocytes.

To date, four similar, high-affinity FGFR genes have been identified from several species [44]. FGFR1–3 are widely expressed in the adult brain and show different cellular locations depending on the region [45]. FGFR1 is

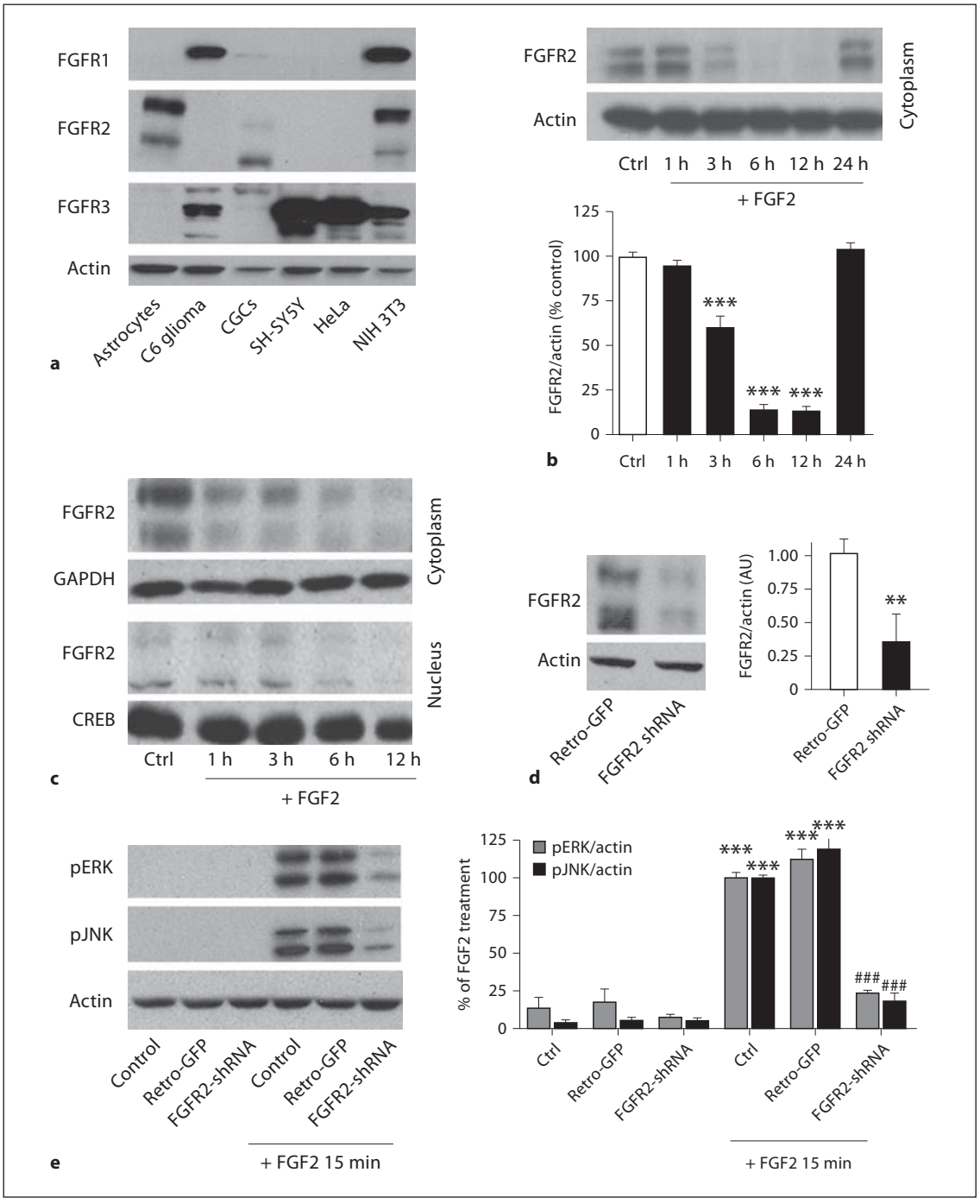

Fig. 6. FGFR2 mediated the immunomodulatory actions of FGF2. **a** Western blot analysis of FGFR1–3 in astrocytes, cerebellar granule cells (CGCs), glioma (C6), SH neuroblastoma, HeLa and NIH3T3. Astrocytes only expressed FGFR2, which appeared in two bands. **b** Western blot analysis of FGFR2 expression in astrocytes upon incubation with FGF2 showing representative blot and densitometry. FGF2 induced the transient disappearance of FGFR2. **c** FGFR2 did not migrate to the nucleus upon FGF2 treatment, as shown in Western blot analysis of cytosolic and nuclear fractions. Protein loading of nuclear fractions was controlled for with CREB expression. The gels show an analysis in subcellular fractions obtained from the same whole-cell extract. **d** Western blot analysis of FGFR2 after overexpressing FGFR2 shRNA, which reduced the expression of the receptor. **e** FGFR2 shRNA completely obliterated pERK and pJNK expression, as shown by Western blot analysis. Data are the means ± SEM of n = 3 independent experiments, except for **c** where a result representative of 2 experiments is shown. * $p < 0.05$, ** $p < 0.01$, *** $p < 0.001$ with respect to control, and ### $p < 0.01$ with respect to Retro-GFP as indicated; ANOVA analysis, Neumann-Keuls post-hoc were used.

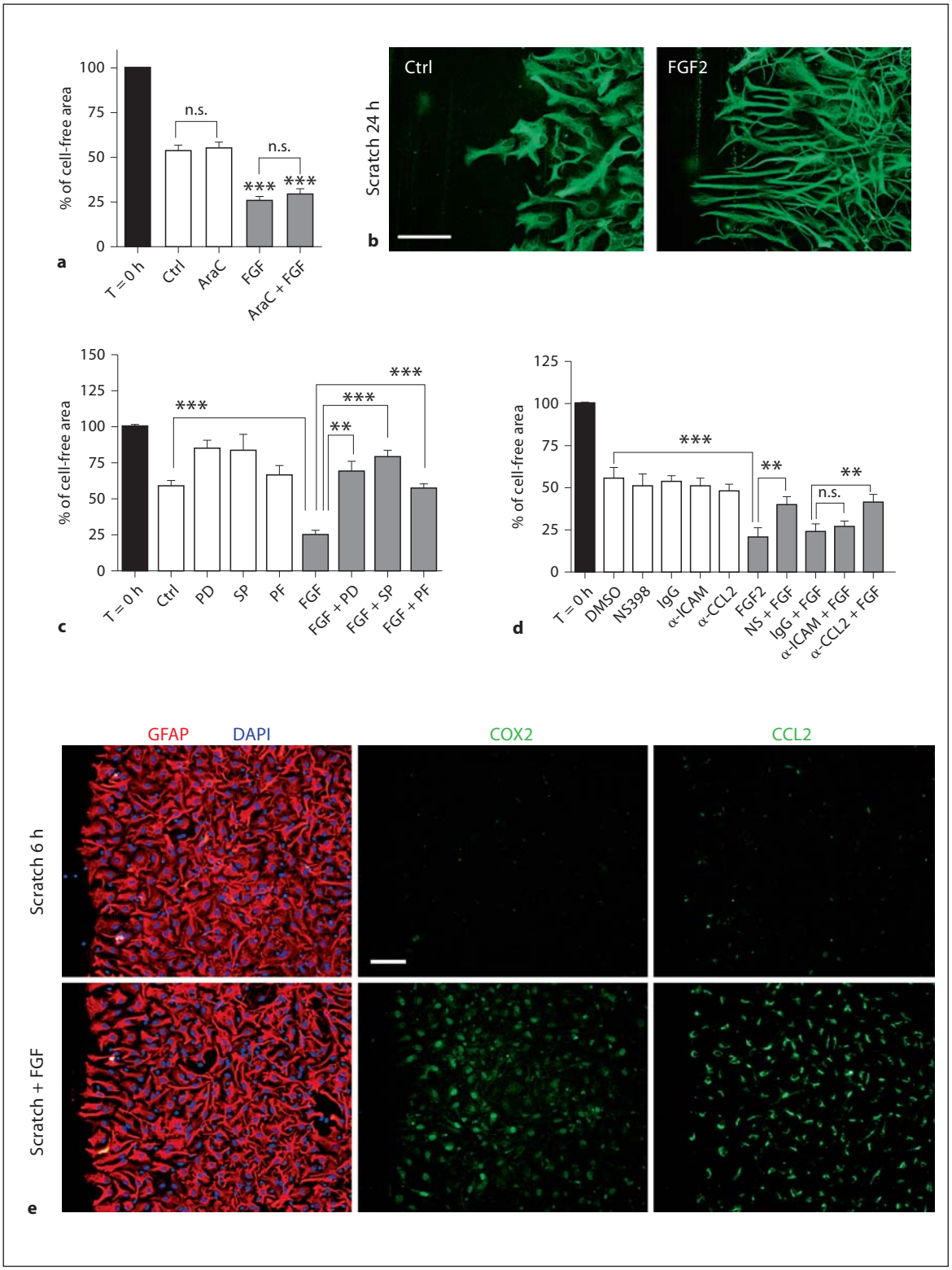

7

(For legend see next page.)

abundant in cortex, hippocampus and cerebellum, while FGFR2 is amply expressed in the olfactory bulb, hippocampus, and cerebellum [46]. Cell-wise, FGFR1 is predominantly expressed in neurons, while FGFR2 and FGFR3 are mainly present in astrocytes [47, 48]. FGFR4, by contrast, is only expressed in early stages of development and, with the exception of the lateral habenular nucleus, is not detectable in the adult brain [49]. In the cerebellar astrocytes used for the present study, we detected FGFR2, but not FGFR1 or 3, indicating that FGFR expression in astrocyte cultures is region specific, that it closely mirrors the distribution described in vivo and that FGFR2 was therefore the receptor type candidate accounting for the observed actions of FGF2. Accordingly, silencing FGFR2 expression by RNA interference led to the blockade of ERK and JNK, the uppermost mediators of FGF2 signaling.

The FGFR1–4 genes encode for structurally similar peptides containing an extracellular domain of three immunoglobulin-like domains, a transmembrane domain and an intracellular tyrosine kinase domain. Cells also exhibit low-affinity FGF-binding sites composed of heparin sulfate proteoglycans [6], which enhance the stability of FGF2-FGFR complexes. The binding of FGF2 to FGFR results in receptor dimerization and autophosphorylation at tyrosine residues. It has been reported that, after the binding of FGF2 to FGFR1, the FGF2-FGR1 complex translocates to the nucleus [50, 51], where it initiates several signaling pathways leading to differentiation and proliferation [8, 52]. Nuclear trafficking of FGF2 and FGFR1 in neurons and astrocytes is indeed a hallmark of injury in the adult brain cortex [19, 20]. However, we found no evidence in the present study that the effect of LMW-FGF2 via FGFR2 involved nuclear actions of the receptor. Western blot analyses showed no signs of nuclear translocation of FGFR2. Rather, a most striking phenomenon was the transient disappearance of FGFR2 in FGF2-stimulated cells, unveiling an inhibitory feedback controlling FGF2-dependent signaling in astrocytes. A comparable phenomenon has been reported in NIH 3T3 cell lines [53], wherein FGFR internalization followed by degradation leads to receptor desensitization. It appears overall that a cell membrane rather than a nuclear FGFR2 accounts for the immunomodulatory actions of LMW-FGF2 in cerebellar astrocytes.

In contrast to FGFR1, the best-characterized FGFR, little is known about the intracellular signaling of FGFR2. For FGFR1, a wealth of evidence documents the activation of three major pathways: phospholipase C/PKC, Ras/MAPK (including ERK, JNK and p38), and PI3K/AKt (for a review, see [54, 55]). While these intracellular signaling cascades have not been confirmed for FGFR2, it is believed that, owing to the strong structural resemblance, the signaling pathways driven by different FGFRs are very similar. Studies with chimeric receptors composed of cytoplasmic domains of FGFR1–4 indeed suggest that the main difference among FGFRs is the strength of tyrosine kinase activity and not the target proteins [56]. No report exists about FGF2-regulating FAK. Since FAK is a key molecule in cell migration (see below), this knowledge gap is consistent with the lack of attention that FGF2 has received as a migration modulator thus far.

We have shown that FAK, JNK and ERK mediate the regulation of CCL2 and ICAM1 by FGF2, while FAK/JNK mediates that of COX2. Downstream effectors remain to be identified, although our data rules out the participation of NF-κB. While a precedent exists of activation of ERK-dependent pathways by FGFR2 [57], the inhibition and not the activation of JNK is involved in the FGF2-mediated protection of myocardial cells from ischemia [58]. This suggests that cells, and not receptors, instruct the particulars of FGF2-elicited signaling. All in all, the data reveal that the various kinases regulating FGF2-mediated immunomodulation interact in a rather complex manner. Firstly, there is gene specificity since ERK regulated CCL2 and ICAM1 but not COX2. Secondly, depending on the target gene, kinases can play both stimulatory (e.g. CCL2 and COX2) and inhibitory

Fig. 7. FGF2 accelerated astrocyte migration in a scratch-injury assay. Effect of FGF2 on the scratch width in the presence or absence of cytosine arabinoside (20 μM) to prevent proliferation (**a**); migration fronts of control and FGF2-treated cells (24 h) stained for GFAP (**b**); effect of PD98059 (50 μM), SP600125 (10 μM) or PF573238 (2.5 μM) on FGF2-induced acceleration (**c**); effect of antibodies blocking CCL2 (αMCP, 4 μg/ml), stimulating ICAM1 (αICAM1, 10 μg/ml), or control unspecific isotype-matched IgG (10 μg/ml), as well as the COX2 inhibitor NS398 (25 μM) (**d**), and control and FGF2-treated (6 h) astrocytes stained for GFAP, CCL2 or COX2 (**e**). In the moving front, FGF2-treated astrocytes adopted a polarized morphology over time, bearing long processes arranged perpendicularly to the scratch. In all experiments, cells were incubated with 25 ng/ml FGF2, and/or the pharmacological inhibitors or αMCP/αICAM1 for the entire time. Migration was measured as the percentage of free area 24 h after the scratch was made. Values are means ± SEM of n = 3–4 independent experiments. * $p < 0.05$, ** $p < 0.01$, *** $p < 0.001$ against control condition unless otherwise noted, ANOVA analysis followed by Neumann-Keuls. Images are representative of 3 independent experiments. Scale bar = 50 μm. FGF2 increased astrocyte acceleration in a fashion dependent on ERK, FAK, JNK, COX2 and CCL2, but not ICAM1.

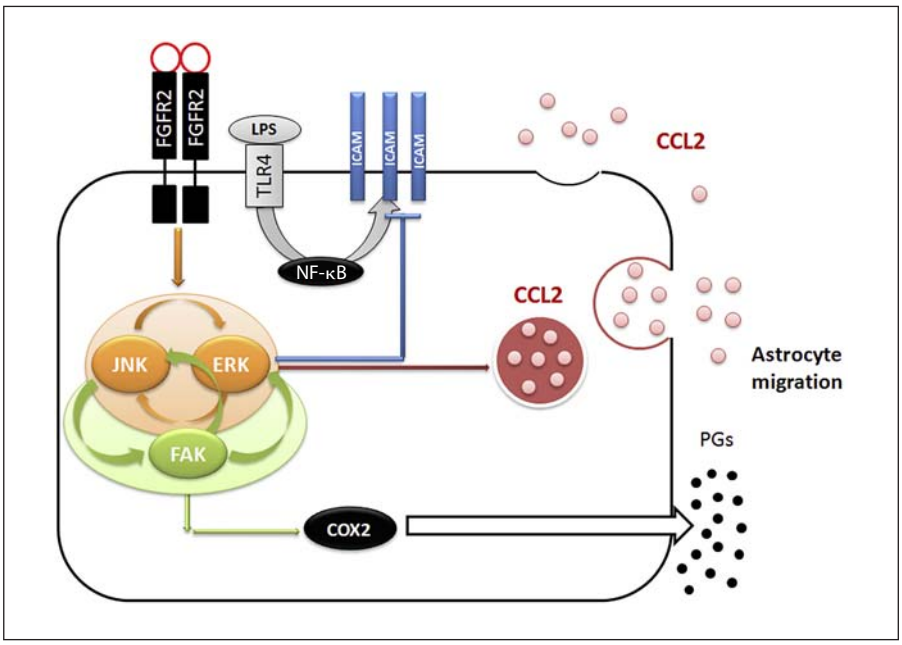

Color version available online

Fig. 8. Schematic representation of FGF2-elicited promigratory signaling pathways in astrocytes. FGF2, acting through FGFR2 receptor, may regulate two kinase loops in astrocytes. One would encompass JNK and ERK and lead to CCL2 synthesis and release, and to the inhibition of LPS-dependent ICAM1 regulation. A second loop would implicate FAK and contribute to: (i) CCL2 and ICAM1 modulation via ERK/JNK and (ii) ERK-independent COX2 upregulation. The delayed and more long-lasting FAK activation suggests a maintenance function of FAK in FGF2 immunomodulatory signaling.

(e.g. ICAM1) roles. Thirdly, examination of hierarchic arrangements with pharmacological kinase inhibitors suggests the existence of intricate feedback loops whereby there is reciprocal regulation of ERK-JNK and FAK-JNK, while FAK stimulates ERK but not the opposite. A schematic consistent with these observations is provided in figure 8. In brief, FGF2 would regulate two intertwined kinase loops in astrocytes. One would encompass JNK and ERK and lead to the stimulation of CCL2 synthesis and release, and also to the inhibition of the LPS-dependent ICAM1 regulation. A second loop would implicate FAK and contribute to: (i) CCL2 and ICAM1 modulation via ERK/JNK and (ii) ERK-independent COX2 upregulation. The delayed and more long-lasting FAK activation with respect to ERK and JNK – as assessed by kinase phosphorylation – suggests a maintenance function of FAK in FGF2 immunomodulatory signaling.

The adaptor protein FAK recruits proteins that regulate the turnover of focal adhesion assemblies during cell migration [59, 60]. The higher the turnover of focal adhesion assemblies, the faster the cell moves. FGF2 has been reported to induce focal adhesion disassembly in brain capillary endothelial cells thus leading to FGF2-directed chemotaxis [61]. The central role of FAK in the FGF2-mediated immunomodulation described in the present study suggests that, like in endothelial cells, the factor may coordinate directed motility in astrocytes through promoting focal adhesion disassembly. Indeed, focal adhesions may contain FGFR [62].

Within focal adhesions, FAK is activated upon ligation of integrins to the extracellular matrix. Integrins, in turn, have been reported to downregulate ICAM1 expression via FAK [63], suggesting that migration requires the downregulation of this adhesion molecule. It was therefore not surprising at first that FGF2 decreased ICAM1 expression while increasing migration via CCL2, all phenomena depending on FAK. We even reasoned that stimulating ICAM1 activity with an anti-ICAM1 antibody would reverse the promigratory actions of FGF2 but, unexpectedly, the antibody had no effect, indicating that the decrease in ICAM1 expression did not contribute to the observed accelerated movement. We speculate that CCL2 and ICAM1 may embody distinct functions of cell adhesion during astrocyte migration upon injury. One is the cell movement along chemotactic gradients, which involves highly controlled cycles of adhesion/deadhesion to the extracellular matrix. Another is the recognition of and the cross-talk with locally activated immune cells, namely microglia. The scratch injury model used in the present study may hence simulate chemotaxis, but not the full range of postinjury immune reactions.

The notion that migration is an integral part of the postinjury inflammatory response in astrocytes has not been recognized, nor the molecular mechanisms dissected out until recently. Thus, it has been reported that

TGFβ, tissue plasminogen activator (tPA) and endothelin stimulate astrocyte migration through metalloprotease-9 (MMP9) [64–66]. The promigratory actions of tPA requires COX2 [65], where those of endothelin involve the nitric oxide-mediated tyrosine nitration of MMP9 [66]. Our study implicates CCL2 and COX2 in the autocrine regulation of astrocyte migration. While CCL2 is a paradigmatic chemotactic agent acting via its receptor CCR2, the mechanisms underlying the promigratory actions of COX2 remain undetermined, although they may involve the interaction of the prostaglandin E_2 with receptor EP1 [67].

Future research will further clarify the molecular signaling guiding astrocyte migration, but for the time being it is worth stressing two ideas. One is that the signaling and the ensuing effects will strictly depend on the stimulating agents. Our data show, for example, that the robust CCL2 expression caused by LPS in astrocytes is not associated with accelerated motion as with FGF2, or that NF-κB does not mediate the effects of FGF2, which is at variance with the reported implication of the transcription factor in the promigratory actions of TGFβ [64]. The other idea is that Rho-GTPases, which play a key role in directed movement in astrocytes by guiding cytoskeleton remodeling [68, 69], are plausible downstream targets of CCL2 and COX2-produced prostaglandins.

It is widely believed that FGF2 is a key regulator of the wounding response in the adult brain. Protective and regenerative effects of FGF2 have been described in brain ischemia [70–72] and spinal cord injury [73, 74]. Plausibly, multiple functions relating to neurons, microvasculature and glia are involved in the beneficial actions of FGF2, but the exact mechanisms of protection are as yet unclear. Likewise, while reactive astrocytes overexpressing FGF2 and FGFRs are an indisputable hallmark of brain injury [18, 20], the role and consequences of astrocyte reactivity are ill defined. In fact, a widespread misconception in the neuroinflammation field is to ascribe roles, generally deleterious, to astrocytes or microglia based exclusively on morphological changes. The existence of a complex, temporally evolving, disease-specific functional heterogeneity in glia after brain injury remains to be fully recognized and characterized. This knowledge void also affects the astrocytes rendered 'reactive' by the in vivo injection of FGF2 to the site of a brain injury [75, 76]. Here we posit that migration of reactive astrocytes to injury sites and eventual formation of a glia limitans lead to repair and tissue regeneration. Recent evidence indeed challenges the prevailing view that astrocyte scars impair tissue repair by hindering axon growth. Firstly, scars are dynamic, highly regulative proteoglycan networks the composition of which can, by controlling the activity of signaling molecules like FGF2, render the microenvironment conducive for axon regeneration [77]. Secondly, astrocyte scars lead to the compaction of microglia and macrophages within necrotic areas thereby preventing inflammation-derived secondary damage [78]. In this study, we have unveiled molecules and signaling pathways contributing to astrocyte migration. Additional molecular profiling of the astrocyte phenotype induced by FGF2 will aid progress towards the understanding, and ultimately the therapeutic utilization, of the repair capability of FGF2 through increasing the migratory ability of astrocytes in the injured brain.

Acknowledgements

The authors want to thank Cristina Gutiérrez and Mar Castillo for expert assistance with astrocyte cultures and immunocytochemical analyses, respectively. The study was supported by BFU2004-00729/BFI and BFU2007-63031/BFI to E.G., and FPI to M.P.L.

References

1 Prats H, Kaghad M, Prats AC, et al: High molecular mass forms of basic fibroblast growth factor are initiated by alternative CUG codons. Proc Natl Acad Sci USA 1989;86:1836–1840.

2 Hardikar AA, Marcus-Samuels B, Geras-Raaka E, Raaka BM, Gershengorn MC: Human pancreatic precursor cells secrete FGF2 to stimulate clustering into hormone-expressing islet-like cell aggregates. Proc Natl Acad Sci USA 2003;100:7117–7122.

3 Dahl JP, Binda A, Canfield VA, Levenson R: Participation of Na,K-ATPase in FGF-2 secretion: rescue of ouabain-inhibitable FGF-2 secretion by ouabain-resistant Na,K-ATPase alpha subunits. Biochemistry 2000;39:14877–14883.

4 Aggarwal S, Gupta S: A possible role for multidrug resistance-associated protein in the secretion of basic fibroblast growth factor by osteogenic sarcoma cell line (MG-63). Int J Oncol 1998;13:1331–1334.

5 Florkiewicz RZ, Anchin J, Baird A: The inhibition of fibroblast growth factor-2 export by cardenolides implies a novel function for the catalytic subunit of Na^+,K^+-ATPase. J Biol Chem 1998;273:544–551.

6 Ibrahimi OA, Zhang F, Hrstka SC, Mohammadi M, Linhardt RJ: Kinetic model for FGF, FGFR, and proteoglycan signal transduction complex assembly. Biochemistry 2004;43:4724–4730.

7 Baldin V, Roman AM, Bosc-Bierne I, Amalric F, Bouche G: Translocation of bFGF to the nucleus is G1 phase cell cycle specific in bovine aortic endothelial cells. EMBO J 1990;9:1511–1517.

8 Bouche G, Gas N, Prats H, Baldin V, Tauber JP, Teissie J, Amalric F: Basic fibroblast growth factor enters the nucleolus and stimulates the transcription of ribosomal genes in ABAE cells undergoing G0–G1 transition. Proc Natl Acad Sci USA 1987;84:6770–6774.
9 Stachowiak EK, Maher PA, Tucholski J, Mordechai E, Joy A, Moffett J, Coons S, Stachowiak MK: Nuclear accumulation of fibroblast growth factor receptors in human glial cells – association with cell proliferation. Oncogene 1997;14:2201–2211.
10 Joy A, Moffett J, Neary K, Mordechai E, Stachowiak EK, Coons S, Rankin-Shapiro J, Florkiewicz RZ, Stachowiak MK: Nuclear accumulation of FGF-2 is associated with proliferation of human astrocytes and glioma cells. Oncogene 1997;14:171–183.
11 Bossard C, Laurell H, Van den Berghe L, Meunier S, Zanibellato C, Prats H: Translokin is an intracellular mediator of FGF-2 trafficking. Nat Cell Biol 2003;5:433–439.
12 Reilly JF, Maher PA: Importin beta-mediated nuclear import of fibroblast growth factor receptor: role in cell proliferation. J Cell Biol 2001;152:1307–1312.
13 Arese M, Chen Y, Florkiewicz RZ, Gualandris A, Shen B, Rifkin DB: Nuclear activities of basic fibroblast growth factor: potentiation of low-serum growth mediated by natural or chimeric nuclear localization signals. Mol Biol Cell 1999;10:1429–1444.
14 Quarto N, Fong KD, Longaker MT: Gene profiling of cells expressing different FGF-2 forms. Gene 2005;356:49–68.
15 Smith C, Berry M, Clarke WE, Logan A: Differential expression of fibroblast growth factor-2 and fibroblast growth factor receptor 1 in a scarring and nonscarring model of CNS injury in the rat. Eur J Neurosci 2001;13:443–456.
16 Cuevas P, Gimenez-Gallego G, Carceller F, Cuevas B, Crespo A: Single topical application of human recombinant basic fibroblast growth factor (rbFGF) promotes neovascularization in rat cerebral cortex. Surg Neurol 1993;39:380–384.
17 Reuss B, Leung DS, Ohlemeyer C, Kettenmann H, Unsicker K: Regionally distinct regulation of astroglial neurotransmitter receptors by fibroblast growth factor-2. Mol Cell Neurosci 2000;16:42–58.
18 do Carmo Cunha J, de Freitas Azevedo Levy B, de Luca BA, de Andrade MS, Gomide VC, Chadi G: Responses of reactive astrocytes containing S100beta protein and fibroblast growth factor-2 in the border and in the adjacent preserved tissue after a contusion injury of the spinal cord in rats: Implications for wound repair and neuroregeneration. Wound Repair Regen 2007;15:134–146.
19 Clarke WE, Berry M, Smith C, Kent A, Logan A: Coordination of fibroblast growth factor receptor 1 (FGFR1) and fibroblast growth factor-2 (FGF-2) trafficking to nuclei of reactive astrocytes around cerebral lesions in adult rats. Mol Cell Neurosci 2001;17:17–30.
20 Leadbeater WE, Gonzalez AM, Logaras N, Berry M, Turnbull JE, Logan A: Intracellular trafficking in neurones and glia of fibroblast growth factor-2, fibroblast growth factor receptor 1 and heparan sulphate proteoglycans in the injured adult rat cerebral cortex. J Neurochem 2006;96:1189–1200.
21 Fahmy GH, Moftah MZ: Fgf-2 in astroglial cells during vertebrate spinal cord recovery. Front Cell Neurosci 2010;4:129.
22 Faber-Elman A, Solomon A, Abraham JA, Marikovsky M, Schwartz M: Involvement of wound-associated factors in rat brain astrocyte migratory response to axonal injury: in vitro simulation. J Clin Invest 1996;97:162–171.
23 Gourmala NG, Buttini M, Limonta S, Sauter A, Boddeke HW: Differential and time-dependent expression of monocyte chemoattractant protein-1 mRNA by astrocytes and macrophages in rat brain: effects of ischemia and peripheral lipopolysaccharide administration. J Neuroimmunol 1997;74:35–44.
24 Yan YP, Sailor KA, Lang BT, Park SW, Vemuganti R, Dempsey RJ: Monocyte chemoattractant protein-1 plays a critical role in neuroblast migration after focal cerebral ischemia. J Cereb Blood Flow Metab 2007;27:1213–1224.
25 Dietrich JB: The adhesion molecule ICAM-1 and its regulation in relation with the blood-brain barrier. J Neuroimmunol 2002;128:58–68.
26 Etienne-Manneville S, Manneville JB, Adamson P, Wilbourn B, Greenwood J, Couraud PO: ICAM-1-coupled cytoskeletal rearrangements and transendothelial lymphocyte migration involve intracellular calcium signaling in brain endothelial cell lines. J Immunol 2000;165:3375–3383.
27 Akiyama H, Kawamata T, Yamada T, Tooyama I, Ishii T, McGeer PL: Expression of intercellular adhesion molecule (ICAM)-1 by a subset of astrocytes in Alzheimer disease and some other degenerative neurological disorders. Acta Neuropathol 1993;85:628–634.
28 Dalmau I, Vela JM, Gonzalez B, Castellano B: Expression of LFA-1alpha and ICAM-1 in the developing rat brain: a potential mechanism for the recruitment of microglial cell precursors. Brain Res Dev Brain Res 1997;103:163–170.
29 Salvador-Silva M, Aoi S, Parker A, Yang P, Pecen P, Hernandez MR: Responses and signaling pathways in human optic nerve head astrocytes exposed to hydrostatic pressure in vitro. Glia 2004;45:364–377.
30 Luo J, Lindstrom CL, Donahue A, Miller MW: Differential effects of ethanol on the expression of cyclo-oxygenase in cultured cortical astrocytes and neurons. J Neurochem 2001;76:1354–1363.
31 Rodriguez C, Lopez P, Pozo M, Duce AM, Lopez-Pelaez M, Fernandez M, Alemany S: COX2 expression and Erk1/Erk2 activity mediate Cot-induced cell migration. Cell Signal 2008;20:1625–1631.
32 Singh B, Berry JA, Shoher A, Ramakrishnan V, Lucci A: Cox-2 overexpression increases motility and invasion of breast cancer cells. Int J Oncol 2005;26:1393–1399.
33 Agullo L, Baltrons MA, Garcia A: Calcium-dependent nitric oxide formation in glial cells. Brain Res 1995;686:160–168.
34 Hao C, Richardsin A, Fedoroff S: Macrophage-like cells originate from neuroepithelium in culture: characterization and properties of the macrophage-like cells. Int J Dev Neurosci 1991;9:1–14.
35 Balyasnikova IV, Pelligrino DA, Greenwood J, Adamson P, Dragon S, Raza H, Galea E: Cyclic adenosine monophosphate regulates the expression of the intercellular adhesion molecule and the inducible nitric oxide synthase in brain endothelial cells. J Cereb Blood Flow Metab 2000;20:688–699.
36 Etienne-Manneville S: In vitro assay of primary astrocyte migration as a tool to study Rho GTPase function in cell polarization. Methods Enzymol 2006;406:565–578.
37 Thompson WL, Van Eldik LJ: Inflammatory cytokines stimulate the chemokine CCL2/MCP-1 and CCL7/MCP-3 through NFκB and MAPK dependent pathways in rat astrocytes. Brain Res 2009;1287:47–57.
38 Heffron Ds, Mandell JW: Opposing role of ERK and p38 MAP kinases in FGF2-induced astroglial process extension. Mol Cell Neurosci 2005;28:779–90.
39 Nugent MA, Iozzo RV: Fibroblast growth factor-2. Int J Biochem Cell Biol 2000;32:115–120.
40 Flinder LI, Timofeeva OA, Rosseland CM, Wierod L, Huifeldt HS, Skarpen E: EGF-induced ERK-activation downstream of FAK requires Rac1-NADPH oxidase. J Cell Physiol 2011;226:2267–2278.
41 Hatch NE, Hudson M, Seto ML, Cunningham ML, Bothwell M: Intracellular retention, degradation, and signaling of glycosylation-deficient FGFR2 and craniosynostosis syndrome-associated FGFR2C278F. J Biol Chem 2006;281:27292–27305.
42 Mangasarian K, Li Y, Mansukhani A, Basilico C: Mutation associated with crouzon syndrome causes ligand-independent dimerization and activation of FGF receptor-2. J Cell Physiol 1997;172:117–125.
43 Madrigal JL, Leza JC, Polak P, Kalinin S, Feinstein DL: Astrocyte-derived MCP-1 mediates neuroprotective effects of noradrenaline. J Neurosci 2009;29:263–267.
44 Johnson DE, Williams LT: Structural and functional diversity in the FGF receptor multigene family. Adv Cancer Res 1993;60:1–41.
45 Belluardo N, Wu G, Mudo G, Hansson AC, Pettersson R, Fuxe K: Comparative localization of fibroblast growth factor receptor-1, -2, and -3 mRNAs in the rat brain: in situ hybridization analysis. J Comp Neurol 1997;379:226–246.

46 Asai T, Wanaka A, Kato H, Masana Y, Seo M, Tohyama M: Differential expression of two members of FGF receptor gene family, FGFR-1 and FGFR-2 mRNA, in the adult rat central nervous system. Brain Res Mol Brain Res 1993;17:174–178.
47 Miyake A, Hattori Y, Ohta M, Itoh N: Rat oligodendrocytes and astrocytes preferentially express fibroblast growth factor receptor-2 and -3 mRNAs. J Neurosci Res 1996;45:534–541.
48 Chadashvili T, Peterson DA: Cytoarchitecture of fibroblast growth factor receptor 2 (FGFR-2) immunoreactivity in astrocytes of neurogenic and non-neurogenic regions of the young adult and aged rat brain. J Comp Neurol 2006;498:1–15.
49 Fuhrmann V, Kinkl N, Leveillard T, Sahel J, Hicks D: Fibroblast growth factor receptor 4 (FGFR4) is expressed in adult rat and human retinal photoreceptors and neurons. J Mol Neurosci 1999;13:187–197.
50 Kilkenny DM, Hill DJ: Perinuclear localization of an intracellular binding protein related to the fibroblast growth factor (FGF) receptor 1 is temporally associated with the nuclear trafficking of FGF-2 in proliferating epiphyseal growth plate chondrocytes. Endocrinology 1996;137:5078–5089.
51 Maher PA: Nuclear translocation of fibroblast growth factor (FGF) receptors in response to FGF-2. J Cell Biol 1996;134:529–536.
52 Stachowiak MK, Fang X, Myers JM, Dunham SM, Berezney R, Maher PA, Stachowiak EK: Integrative nuclear FGFR1 signaling (INFS) as a part of a universal 'feed-forward-and-gate' signaling module that controls cell growth and differentiation. J Cell Biochem 2003;90:662–691.
53 Moscatelli D, Devesly P: Turnover of functional basic fibroblast growth factor receptors on the surface of BHK and NIH 3T3 cells. Growth Factors 1990;3:25–33.
54 Wiedlocha A, Sorensen V: Signaling, internalization, and intracellular activity of fibroblast growth factor. Curr Top Microbiol Immunol 2004;286:45–79.
55 Beenken A, Mohammadi M: The FGF family: biology, pathophysiology and therapy. Nat Rev Drug Discov 2009;8:235–253.
56 Raffioni S, Thomas D, Foehr ED, Thompson LM, Bradshaw RA: Comparison of the intracellular signaling responses by three chimeric fibroblast growth factor receptors in PC12 cells. Proc Natl Acad Sci USA 1999;96:7178–7183.
57 Miraoui H, Oudina K, Petite H, Tanimoto Y, Moriyama K, Marie PJ: Fibroblast growth factor receptor 2 promotes osteogenic differentiation in mesenchymal cells via ERK1/2 and protein kinase C signaling. J Biol Chem 2009;284:4897–4904.
58 Liao S, Porter D, Scott A, Newman G, Doetschman T, Schultz Jel J: The cardioprotective effect of the low molecular weight isoform of fibroblast growth factor-2: the role of JNK signaling. J Mol Cell Cardiol 2007;42:106–120.
59 Tomar A, Schlaepfer DD: Focal adhesion kinase: switching between GAPs and GEFs in the regulation of cell motility. Curr Opin Cell Biol 2009;21:676–683.
60 Laczko R, Szauter KM, Jansen MK, Hollosi P, Muranyi M, Molnar J, Fong KS, Hinek A, Csiszar K: Active lysyl oxidase (LOX) correlates with focal adhesion kinase (FAK)/paxillin activation and migration in invasive astrocytes. Neuropathol Appl Neurobiol 2007;33:631–643.
61 Kanda S, Miyata Y, Kanetake H, Smithgall TE: Fibroblast growth factor-2 induces the activation of Src through Fes, which regulates focal adhesion disassembly. Exp Cell Res 2006;312:3015–3022.
62 Lehembre F, Yilmaz M, Wicki A, Schomber T, Strittmatter K, Ziegler D, Kren A, Went P, Derksen PW, Berns A, Jonkers J, Christofori G: NCAM-induced focal adhesion assembly: a functional switch upon loss of E-cadherin. EMBO J 2008;27:2603–2615.
63 Yasuda M, Tanaka Y, Tamura M, Fujii K, Sugaya M, So T, Takenoyama M, Yasumoto K: Stimulation of beta1 integrin down-regulates ICAM-1 expression and ICAM-1-dependent adhesion of lung cancer cells through focal adhesion kinase. Cancer Res 2001;61:2022–2030.
64 Hsieh HL, Wang HH, Wu WB, Chu PJ, Yang CM: Transforming growth factor-β1 induces matrix metalloproteinase-9 and cell migration in astrocytes: roles of ROS-dependent ERK- and JNK-NF-κB pathways. J Neuroinflammation 2010;7:88.
65 Chiu WT, Shen SC, Chow JM, Lin CW, Shia LT, Chen YC: Contribution of reactive oxygen species to migration/invasion of human glioblastoma cells U87 via ERK-dependent cox-2/PGE(2) activation. Neurobiol Dis 2010;37:118–129.
66 Wang HH, Hsieh HL, Yang CM: Nitric oxide production by endothelin-1 enhances astrocytic migration via the tyrosine nitration of matrix metalloproteinase-9. J Cell Physiol 2011;226:2244–2256.
67 Yang SF, Chen MK, Hsieh YS, Chung TT, Hsieh YH, Lin CW, Su JL, Tsai MH, Tang CH: Prostaglandin E2/EP1 signaling pathway enhances intercellular adhesion molecule 1 (ICAM-1) expression and cell motility in oral cancer cells. J Biol Chem 2010;285:29808–29816.
68 Etienne-Manneville S: Polarity proteins in glial cell functions. Curr Opin Neurobiol 2008;18:488–494.
69 Lichtenstein MP, Carriba P, Baltrons MA, Wojciak-Stothard B, Peterson JR, Garcia A, Galea E: Secretase-independent and Rho GTPase/PAK/ERK-dependent regulation of cytoskeleton dynamics in astrocytes by NSAIDs and derivatives. J Alzheimers Dis 2010;22:1135–1155.
70 Bethel A, Kirsch JR, Koehler RC, Finklestein SP, Traystman RJ: Intravenous basic fibroblast growth factor decreases brain injury resulting from focal ischemia in cats. Stroke 1997;28:609–615.
71 Martinez G, Di Giacomo C, Sorrenti V, Carnazza ML, Ragusa N, Barcellona ML, Vanella A: Fibroblast growth factor-2 and transforming growth factor-beta1 immunostaining in rat brain after cerebral postischemic reperfusion. J Neurosci Res 2001;63:136–142.
72 Kiprianova I, Schindowski K, von Bohlen und Halbach O, Krause S, Dono R, Schwaninger M, Unsicker K: Enlarged infarct volume and loss of BDNF mRNA induction following brain ischemia in mice lacking FGF-2. Exp Neurol 2004;189:252–260.
73 Furukawa S, Furukawa Y: FGF-2-treatment improves locomotor function via axonal regeneration in the transected rat spinal cord (in Japanese). Brain Nerve 2007;59:1333–1339.
74 Tripathi RB, McTigue DM: Chronically increased ciliary neurotrophic factor and fibroblast growth factor-2 expression after spinal contusion in rats. J Comp Neurol 2008;510:129–144.
75 Barotte C, Eclancher F, Ebel A, Labourdette G, Sensenbrenner M, Will B: Effects of basic fibroblast growth factor (bFGF) on choline acetyltransferase activity and astroglial reaction in adult rats after partial fimbria transection. Neurosci Lett 1989;101:197–202.
76 Eclancher F, Kehrli P, Labourdette G, Sensenbrenner M: Basic fibroblast growth factor (bFGF) injection activates the glial reaction in the injured adult rat brain. Brain Res 1996;737:201–214.
77 Kasai M, Jikoh T, Fukumitsu H, Furukawa S: FGF-2-responsive and spinal cord-resident cells improve locomotor function after spinal cord injury. J Neurotrauma 2010, E-pub ahead of print.
78 Renault-Mihara F, Okada S, Shibata S, Nakamura M, Toyama Y, Okano H: Spinal cord injury: emerging beneficial role of reactive astrocytes' migration. Int J Biochem Cell Biol 2008;40:1649–1653.